Engineering Fracture Mechanics 199 (2018) 658–671

Contents lists available at ScienceDirect

Engineering Fracture Mechanics

journal homepage: www.elsevier.com/locate/engfracmech

Normalization method for *J*-R curve determination using SENT specimens

João Teixeira Oliveira de Menezes[a,*], Juan E. Perez Ipiña[b], Enrique M. Castrodeza[a]

[a] Laboratory of Fracture Mechanics, COPPE/Federal University of Rio de Janeiro, P.O. Box 68505, Rio de Janeiro, RJ 21941-972, Brazil
[b] Fracture Mechanics Group, National University of Comahue/CONICET, 1400 Buenos Aires St., Neuquén Q8300IBX, Argentina

ARTICLE INFO

Keywords:
Structural steels
J-R curves
SENT geometry
Normalization method

ABSTRACT

According to BS 8571:2014, standard *J*-R curves from SENT geometry can be determined from single or multiple specimens. The recommended methodologies for single specimen include unloading compliance or DCPD, although any validated technique can be used. The normalization method, which is not directly recommended in BSI standards, is an alternative. *J*-R curves through normalization technique based on *P*-CMOD records were experimentally determined using SENT specimens ($0.40 < a_0/W < 0.55$) of two structural steels, later compared with the ones measured by unloading compliance. Results indicated that the normalization method is a valid alternative for *J*-R curve determination using SENT specimens.

1. Introduction

Structural integrity assessment of cracked components and structures needs the fracture mechanics properties, which must be experimentally measured. In general, ductile materials require the application of elastic-plastic methodologies, such as CTOD (δ) or *J*-Integral (*J*), to characterize the fracture toughness. Normally, the crack driving force is measured as a function of stable crack extension, resulting in δ-R or *J*-R curves. The crack-tip constraint level due to a/W, specimen geometry and/or loading type strongly affects the R-curves. High constraint specimens limit plasticity, lead to expected conservative values of fracture toughness, and tend to present lower R-curves, whereas low-constraint specimens produce higher R-curves for the same material [1–3]. The widely known ASTM E1820-17a [4] and BS 7448-4:1997 [5] standards require high constraint three-point bending specimens, SE(B), or compact tension specimens, C(T) or DC(T), containing deep, through-the-thickness cracks with $a/W \geq 0.5$, resulting in lower R-curves. When the structural integrity of cracked pipes containing a circumferential flaw are analyzed, these curves and the associated fracture toughness values could be overly conservative.

In 2003, Nyhus et al. [6] showed that a pipe containing a circumferential flaw subjected to bending efforts presents the crack-tip in low constraint condition and proved that Single Edge Notched Tension – SENT – specimens represent this situation more realistically than SE(B) and C(T) specimens. Other investigations were performed on pin-loaded and clamped SENT specimens, and it was verified that the crack-tip constraint level was similar to an axial surface crack in a pipe with identical crack length and a circumferential surface crack with identical length in a pipeline under combined loading, respectively [7,8]. In this context, SENT specimens are capable of reproducing crack-tip constraint conditions similar to axial and circumferential cracks in a pipeline. Therefore, this geometry could be preferred for the determination of crack growth resistance curves of pipes in laboratory tests, as it seems to be more representative of the material behavior in real operational conditions.

Det Norske Veritas (DNV) [9] and Canada Centre for Mineral and Energy Technology (CanMet) [10–12] developed testing

* Corresponding author.
E-mail address: joaotom@metalmat.ufrj.br (J.T.O.d. Menezes).

https://doi.org/10.1016/j.engfracmech.2018.06.033
Received 22 March 2018; Received in revised form 21 June 2018; Accepted 25 June 2018
Available online 26 June 2018

Nomenclature

a	crack length
a_0	initial crack length
a_{bi}	blunting corrected crack size at *i*th data point
a_f	final crack length
b_0	initial remaining ligament
B	specimen thickness
B_e	effective specimen thickness
C_{CMOD}	specimen elastic compliance based on *P*-CMOD record
C(T)	compact tension specimen
DC(T)	disk-shaped compact specimens
E	Young's modulus of elasticity
E'	effective Young's modulus of elasticity and for plane strain conditions, the appropriate effective elastic modulus is $E' = E/(1 - \upsilon^2)$
H	distance between clamped grips
J	*J*-Integral
$J_{0.2BL}$	resistance to crack extension at 0.2 mm crack extension offset to the blunting line of BSI standards
$J_{0.2}$	resistance to crack extension at 0.2 mm crack extension including blunting
$J_{1.0}$	*J*-Integral value at $\Delta a = 1.0$ mm
J_{el}	elastic component of *J*-Integral
J_{Ic}	crack-extension resistance at 0.2 mm crack extension offset to the blunting line of ASTM standards
J_{pl}	plastic component of *J*-Integral
K_I	elastic stress intensity factor
m	constraint factor
n	Ramberg-Osgood strain hardening exponent
P	nominal force
P_N	normalized force
R-curve	crack growth resistance curve
SE(B)	Single edge-notched bending specimen
SENT	Single edge-notched tension specimen
U_p	plastic work calculated from the area under the *P*-CMOD record
W	specimen width
δ	crack-tip opening displacement (CTOD)
Δa	crack extension
η_p	non-dimensional parameter dependent of geometry and loading type that relates the plastic contribution of *J*-integral to the work per unit uncracked ligament area in loading a cracked body
υ	Poisson's ratio
σ_{UTS}	ultimate tensile strength
σ_Y	effective yield strength
σ_{YS}	0.2% offset yield strength

Abbreviations

CMOD	crack mouth opening displacement
HSLA	high strength low alloy steel
LLD, v	load line displacement
NT	normalization technique
THS	tough high strength steel
UC	unloading compliance method

procedures to measure fracture toughness using SENT specimens. Recently, the British Standard Institution (BSI) released the BS 8571:2014 standard [13] to determine fracture toughness for SENT specimens. All methods need that force (P), and crack mouth opening displacement (CMOD) are continuously measured during tests.

There are several single-specimen methodologies to determine *J*-R curves, normalization technique and elastic unloading compliance method are some of them and have been adopted in ASTM E1820 standard.

Initially, use of the normalization technique was proposed without the necessity of implementing specific instrumentation (i.e. fracture extensometers). Thereby, *J*-R curves could be obtained through load vs. load-line displacement records (*P*-LLD) and initial and final physical crack lengths measured from fracture surfaces. This methodology is based on the load separation principle introduced by *Ernst et al.* [14]. Later, other researchers also investigated it [15–18]. They demonstrated that, in some cases, load can be separated in two multiplicative functions, one dependent on crack length – $G(a/W)$ – and the other dependent on plastic displacement – $H(v_{pl}/W)$ – as follows:

$$P = G(a/W)H(v_{pl}/W). \tag{1}$$

According to this equation, a relationship between the three variables P, a and v, can be inferred during tests [19–22]. Dividing load by function G, P acquires the normalized form (P_N) and is defined in terms of plastic displacement or, in other words, in terms of the material plastic behavior:

$$P_N = \frac{P}{G(a/W)} = H(v_{pl}/W). \tag{2}$$

The function H is currently expressed as a function of four parameters (a, b, c and d) [23], see Eq. (6), and the appropriated constants for each specimen can be fitted through some data pairs of points of normalized load vs. normalized plastic displacement record ($P_N - v_{pl}/W$). Then, using the fitted normalization function, the crack extension can be evaluated iteratively at all loading points for each specimen [24–26]. This methodology is standardized by ASTM (ASTM E1820 standard), which allows tests only in SE (B), C(T) and DC(T) specimens containing deep cracks ($0.45 \le a/W \le 0.7$).

In this investigation, the normalization technique was applied to SENT specimens ($0.40 < a_0/W < 0.55$) of two types of structural steels to obtain the corresponding *J*-R curves. Some modifications to the standard methodology were applied, as the use of *P*-CMOD record instead of *P*-LLD ones. The measured *J*-R curves were compared to those obtained from the same specimens by the unloading compliance technique.

2. Materials and methods

2.1. Materials

Two different structural steels were tested, a high strength low alloy steel (HSLA) and a tough high strength steel (named in this investigation as THS). For the first material, two specimens were tested and for the latter five specimens were used. To obtain the tensile mechanical properties for both materials, tensile tests according to ASTM E8/E8M-15a [27] were performed in cylindrical standardized specimens. Table 1 presents the tensile mechanical properties of the materials.

2.2. Fracture testing

Fracture toughness tests were performed on SENT specimen geometry according to BS 8571:2014 standard (C-type specimen, $W/B = 0.5$), in air, at room temperature and under displacement control. An Instron 1332 servo-hydraulic testing machine instrumented with ± 250 kN load cell and a MTS 632.03F-31 fracture extensometer with 12 mm of nominal travel were used. The nominal dimensions of SENT specimens with integral knife edges can be seen in Fig. 1. All specimens were fatigue pre-cracked in a three-point bending device under a load ratio $R = 0.1$ at approximately 20 Hz. The maximum pre-cracking load for each specimen was calculated according to ASTM E1820-17a.

2.3. Crack length measurement

Crack lengths were evaluated through normalization technique and by elastic unloading compliance, the latter being used as a reference. A brief explanation of each technique follows, including the modifications employed.

2.3.1. Normalization method

Although use of the method was proposed on *P*-LLD records, in this investigation the normalization technique was applied on load vs. crack mouth opening displacement records (*P*-CMOD). Afterwards, on the *Discussion* section, the use of *P*-CMOD records will be justified. The application of the method was based on two standards procedures: Annex 15 of ASTM E1820-17a standard and BS8571:2014 standard, which were slightly modified. The main methodology including modifications is briefly described below.

Initially each P_i value up to, but not including, the maximum force $P_{\max}$, of each experimental *P*-CMOD record is normalized using Eq. (3).

$$P_{Ni} = \frac{P_i}{WB\left(\frac{W-a_{bi}}{W}\right)^{\eta_p}}, \tag{3}$$

where i refers to the ith loading point. In this work the value of η_{p} was calculated as given by Eq. (10) in BS 8571:2014 standard, and a_{bi} is the blunting corrected crack size at ith data point calculated by the following equation:

$$a_{bi} = a_0 + \frac{J_i}{2m\sigma_Y}. \tag{4}$$

The applicability of Eq. (4) to SENT specimens, as well as the use of an m factor in it, will be discussed later. For the corresponding CMOD, a normalization procedure is necessary to give a normalized plastic CMOD. The plastic component of CMOD is then normalized as:

$$\mathrm{CMOD}'_{pl,i} = \frac{\mathrm{CMOD}_{pl,i}}{W} = \frac{\mathrm{CMOD}_i - P_i C_{\mathrm{CMOD},i}}{W}, \tag{5}$$

where $\mathrm{CMOD_{pl,i}}$ is the plastic component of CMOD, CMOD_i is the total crack mouth opening displacement, and $C_{\mathrm{CMOD},i}$ is the specimen elastic crack mouth opening displacement compliance based on the corrected blunted crack size a_{bi}.

The final P and CMOD data pair is normalized using the same equations as described above, with the final physical crack length measured from the fracture surface. Thereafter, the normalized data is plotted and a tangent line from the final load-displacement pair to the curve must be drawn. The data to the right of the tangency point shall be excluded for the fitting procedure. Normalized data with plastic normalized CMOD lower than 0.001 must be also excluded. Thus, through the following normalization function expressed by Eq. (6), remaining data can be fitted.

Table 1
Yield strength (σ_{YS}), ultimate tensile strength (σ_{UTS}) and the strain hardening exponent (n) of the studied structural steels (MPa).

Material	σ_{YS}	σ_{UTS}	n
HSLA steel	396	500	8
THS steel	786	853	10

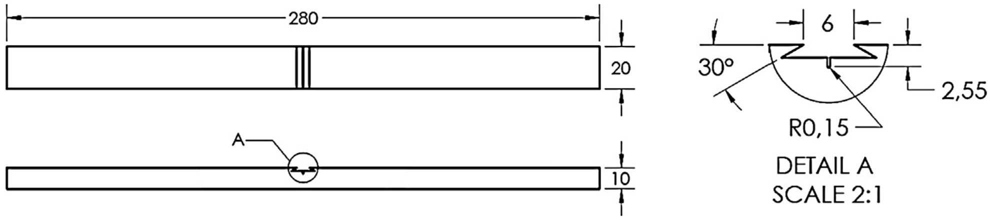

Fig. 1. SENT fracture specimen geometry. In detail, the profile of the notch.

$$P_N = \frac{a+bCMOD'_{pl} + cCMOD'_{pl}}{d+CMOD'_{pl}}, \tag{6}$$

where a, b, c and d are fitting constants. Finally, through the fitted normalization function, an iterative procedure is used adjusting crack lengths a_i to force P_{Ni} and $CMOD'_{pli}$ defined by Eq. (6) to be equal to P_{Ni} and $CMOD'_{pli}$ described by Eqs. (3) and (5), respectively. The a_i that best fit Eq. (6) to the experimental data is the instantaneous estimative of the physical crack length used for *J*-R curves determination.

2.3.2. Unloading compliance method

Crack lengths by unloading compliance were estimated through the compliance equation given by *Cravero and Ruggieri* [28] valid for clamped SENT specimen with $H/W = 10$ and integral knife edges:

$$\frac{a}{W} = 1.6485 - 9.1005u + 33.025u^2 - 78.467u^3 + 97.344u^4 - 47.227u^5, \tag{7}$$

where

$$u = \frac{1}{1 + \sqrt{B_e C_{CMOD} E'}}. \tag{8}$$

This equation is valid over the range $0.1 \le a/W \le 0.7$.

2.4. J-Integral calculations

J-Integral values were calculated according to BS 8571:2014 standard [13] as:

$$J = J_{el} + J_{pl}. \tag{9}$$

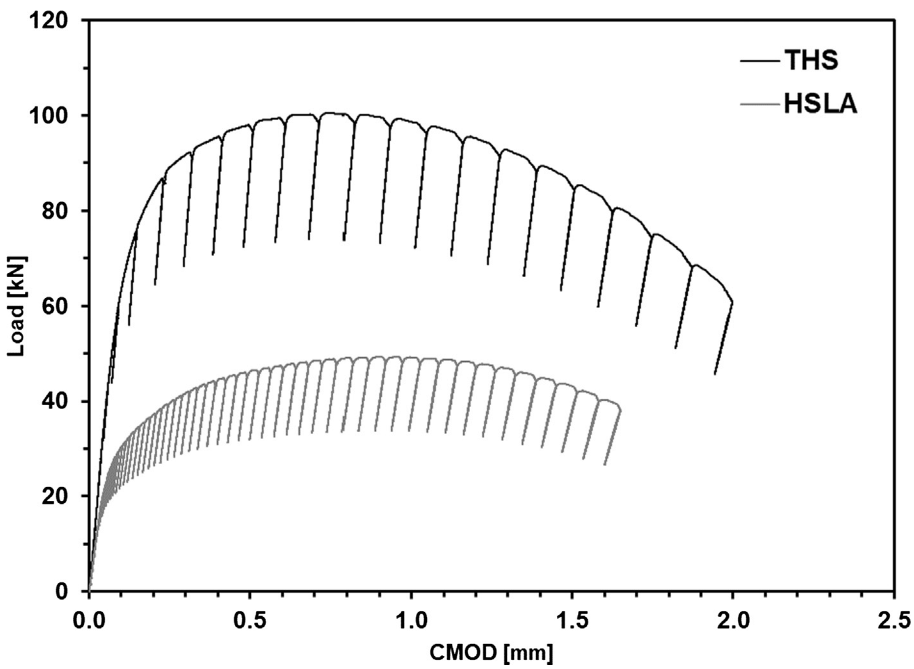

Fig. 2. Typical *P*-CMOD records for the tested materials in SENT geometry.

where

$$J_{el} = \frac{K_I^2(1-\upsilon^2)}{E}, \quad (10)$$

K_I is the stress intensity factor. The plastic component of J-Integral was calculated according to the following equation:

$$J_{pl} = \frac{\eta_p U_p}{B(W-a_0)}, \quad (11)$$

With η_p calculated in terms of CMOD as given by Eq. (10) of this standard.

3. Results

3.1. P-CMOD records

Typical experimental load (P) vs. crack mouth opening displacement (CMOD) records for the tested materials are shown in Fig. 2. The unloading/reloading sequences corresponding to the unloading compliance method are clearly seen in these records.

3.2. Crack length measurements

The initial and final physical crack lengths were measured from the fracture surfaces using the 9-point average method as described in BS 7448-1:1991 standard [29]. Figs. 3 and 4 present typical fracture surfaces of the SENT specimens for HSLA and THS steel respectively. The fatigue pre-cracked region and the stable crack growth region are clearly seen, as well as the fatigue and the stable crack growth fronts, which were very regular in all cases.

Initial a_0/W ratio, final crack length, physical (Δa) and unloading compliance (Δa_{UC}) stable crack extensions, as well as the percentage difference between them for each specimen are shown in Table 2. None of the tests became invalid as a result of irregular fatigue crack front and/or crack growth.

3.3. Normalized functions

Each P-CMOD record was normalized using Eqs. (3)–(6). These data are plotted in Figs. 5 and 6, as well as the fitted curves (in red) obtained using only the dark points. In these figures, it is also possible to see the fitting coefficients for the normalization calibration function of these specific specimens.

3.4. Calculations of crack extension

Crack extensions by both methodologies were calculated as described in *Materials and Methods*. Figs. 7 and 8 present comparisons of crack extension values by normalization and by elastic unloading compliance for HSLA and THS steel specimens, respectively. To assist further analysis, the identity line was also plotted in both figures.

3.5. J-R curves

Figs. 9 and 10 show typical experimental $J - \Delta a$ pairs from each test by normalization technique (NT) and by elastic unloading compliance method (UC). The first one represents a typical J-R curve of the HSLA steel and the second one of the THS steel. Vertical auxiliary lines at 0.2 mm and at 20% of b_0 in Δa were additionally plotted in both figures. Blunting lines as proposed by BS 7448-4:1997 standard were also drawn (although the concept of blunting line is not used in the BS 8571:2014 standard).

Figs. 11 and 12 present all experimental $J - \Delta a$ pairs obtained through normalization technique and elastic unloading compliance method for HSLA and THS steel, respectively.

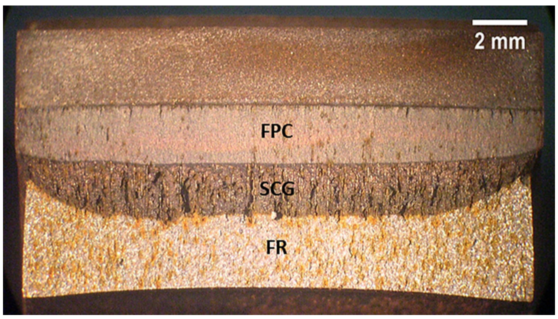

Fig. 3. Typical fracture surface of HSLA steel. FPC: fatigue pre-crack; SCG: stable crack growth; FR: final post-test brittle fracture.

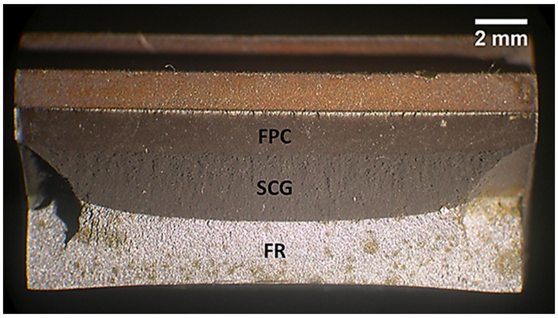

Fig. 4. Typical fracture surface of THS steel. FPC: fatigue pre-crack; SCG: stable crack growth; FR: final post-test brittle fracture.

Table 2
Initial (a_0) and final (a_f) crack lengths, physical (Δa) and unloading compliance (Δa_{UC}) stable crack extensions of each tested specimen.

Material	Specimen	a_0/W (mm)	a_f (mm)	Δa (mm)	Δa_{UC} (mm)	Diff. (%)
HSLA steel	01	0.525	6.71	1.49	1.45	2.68
	02	0.515	8.13	2.98	2.88	3.36
THS steel	01	0.412	6.34	2.16	2.10	2.78
	02	0.466	7.55	2.42	2.11	12.81
	03	0.427	6.60	2.34	2.27	2.99
	04	0.426	[a]	[a]	1.10	[a]
	05	0.415	6.47	2.31	2.39	3.46

[a] After the test and prior to heat tinting this specimen was accidentally broken.

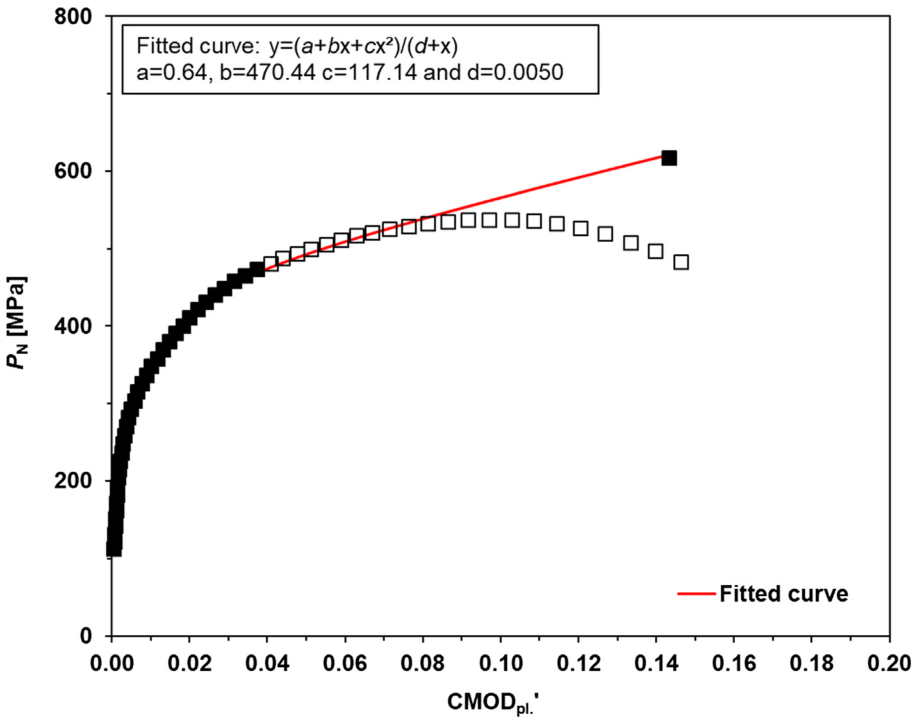

Fig. 5. Normalized load vs. normalized plastic crack mouth opening displacement for SENT 01 of HSLA steel.

3.6. Initiation fracture toughness determination

Strictly speaking, the standardized determination of initiation fracture toughness for SENT specimens can only be made through the BS 8571:2014 standard. In this standard the initiation value of fracture toughness of the material ($J_{0.2}$) is defined as the value of J at 0.2 mm of crack extension from the R-curve fit [13]. For comparison, similar toughness values were also determined through

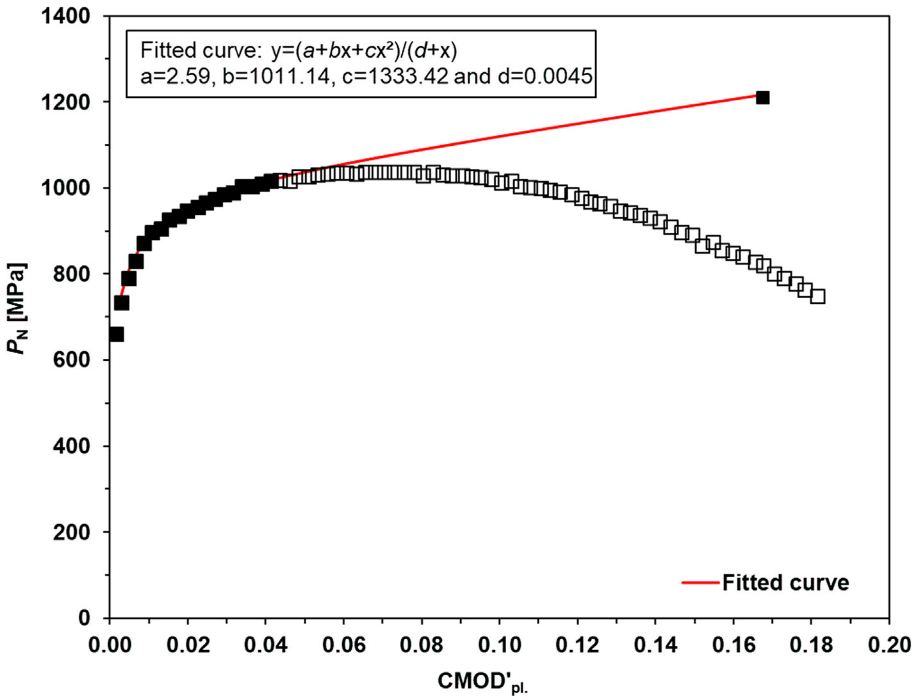

Fig. 6. Normalized load vs. normalized plastic crack mouth opening displacement for SENT 02 of THS steel.

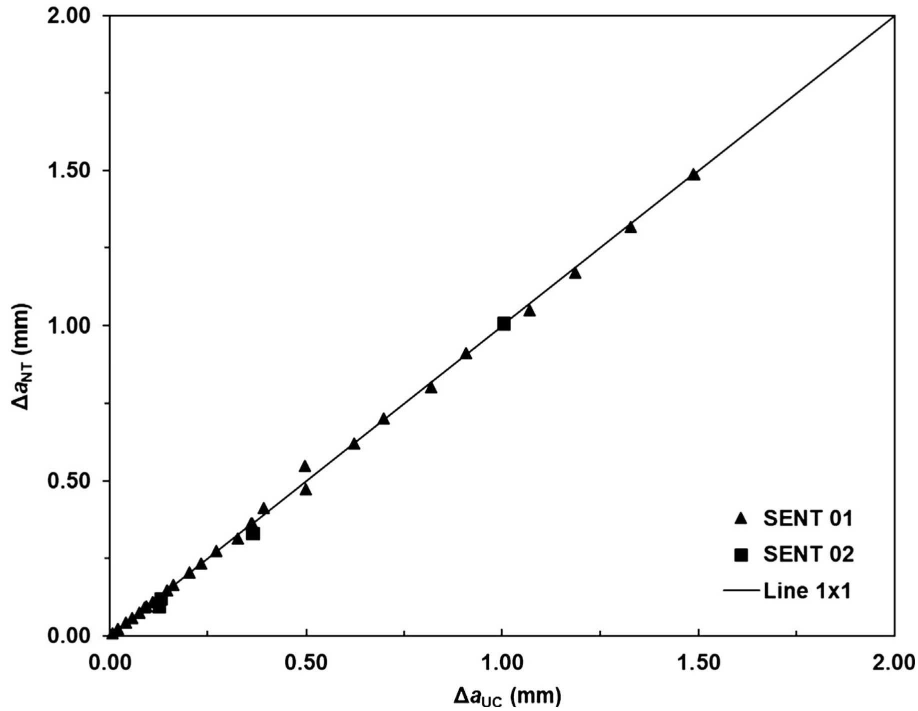

Fig. 7. Comparison of crack extensions obtained through normalization technique and elastic unloading compliance method for specimens of HSLA steel.

procedures described in ASTM E1820–17a (J_{Ic}) and BS 7448-4:1997 ($J_{0.2BL}$) standards, which include the concept of blunting line. As initiation fracture toughness is defined at the interception of J-R curves with an auxiliary line, a best fit procedure is necessary to obtain the fracture toughness values. In this investigation, the equation used to fit the qualified data was the one described in BS 8571:2014. Tables 3 and 4 present toughness values of both materials obtained by normalization technique and unloading

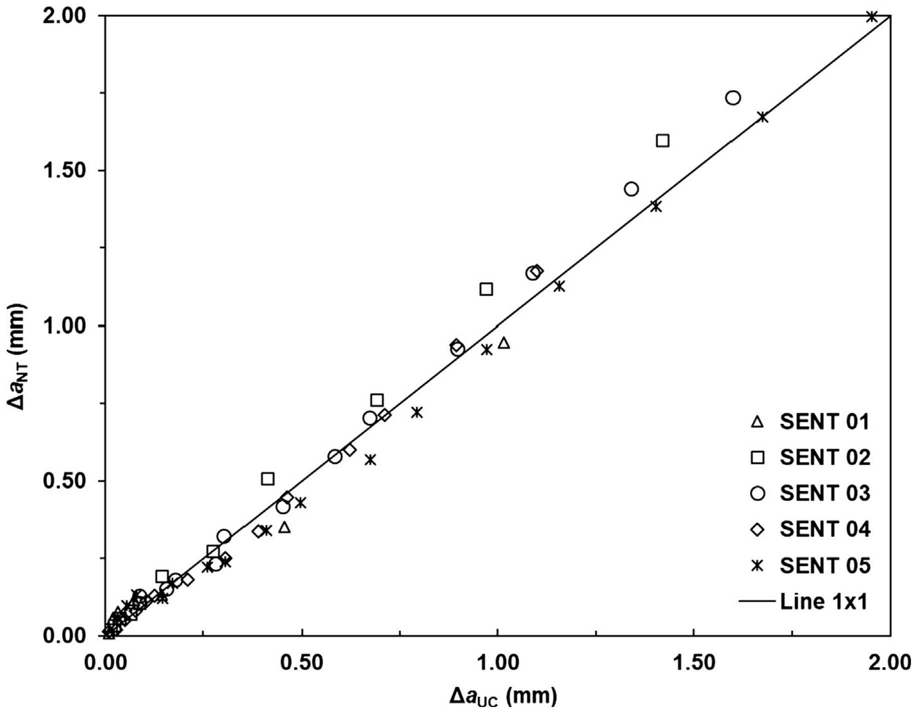

Fig. 8. Comparison of crack extensions obtained through normalization technique and elastic unloading compliance method for specimens of THS steel.

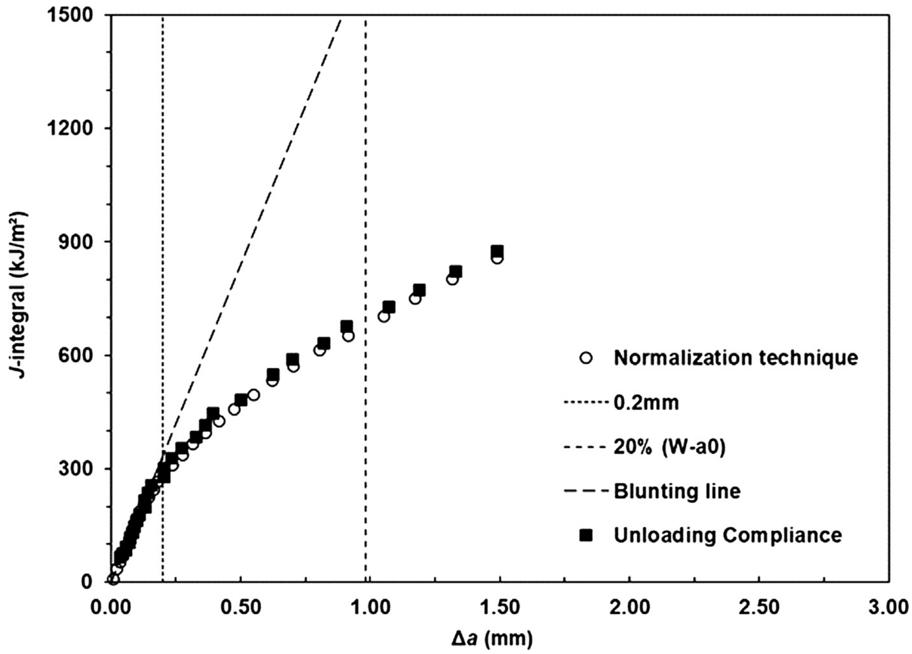

Fig. 9. Experimental $J - \Delta a$ pairs obtained by NT and UC for SENT 01 of HSLA steel.

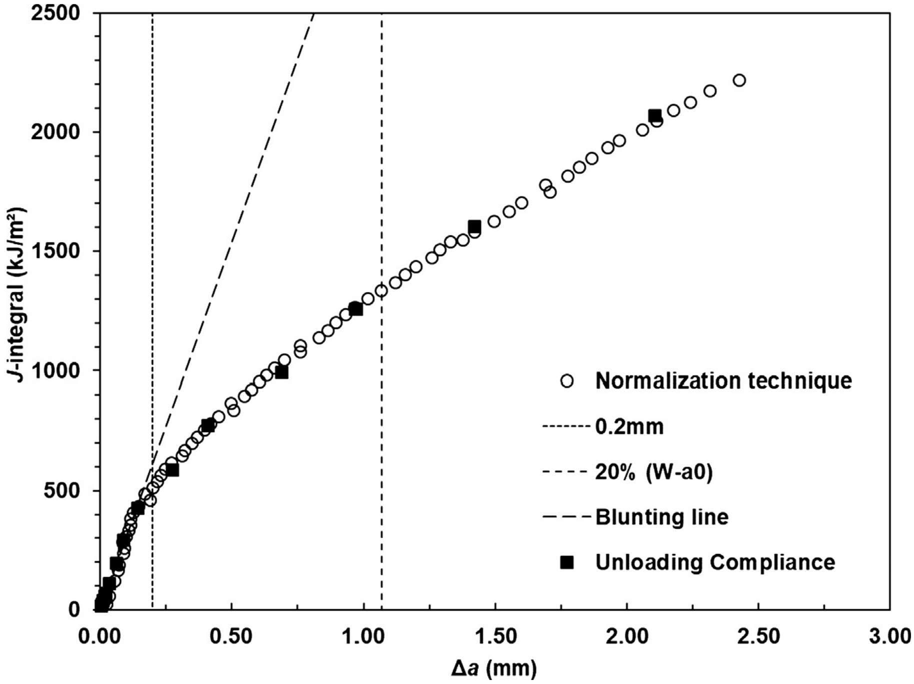

Fig. 10. Experimental $J - \Delta a$ pairs obtained by NT and UC for SENT 02 of THS steel.

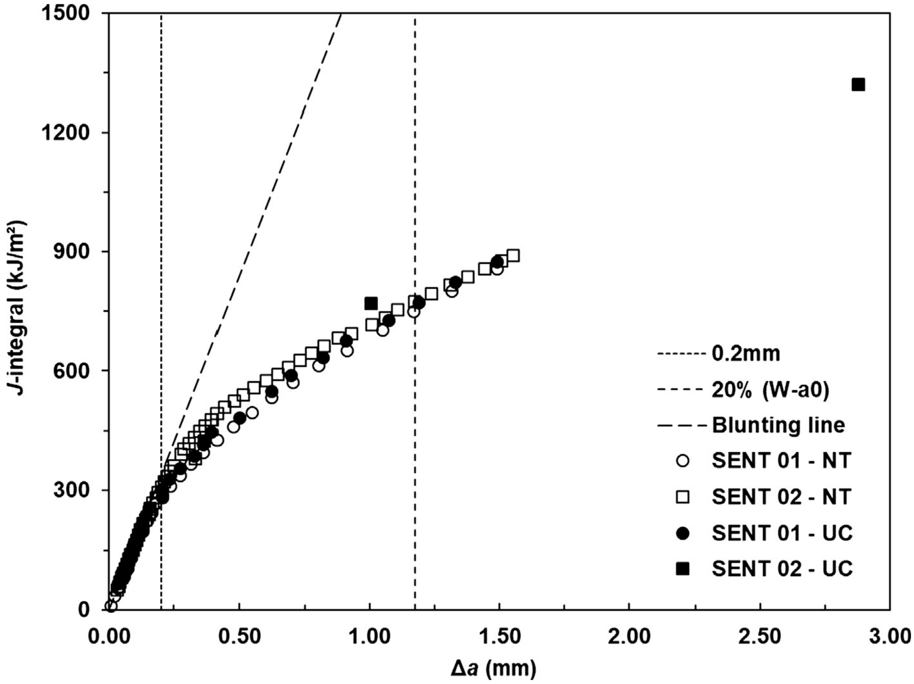

Fig. 11. Comparison of experimental $J - \Delta a$ pairs obtained through unloading compliance method (UC) and normalization technique (NT) for the SENT specimens of HSLA steel.

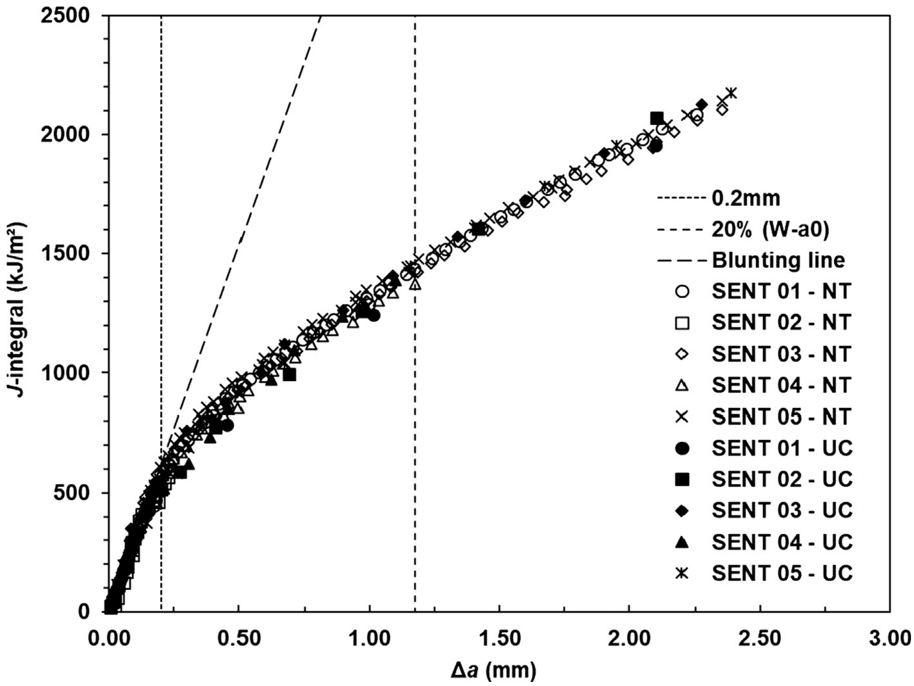

Fig. 12. Comparison of experimental $J - \Delta a$ pairs obtained through unloading compliance method (UC) and normalization technique (NT) for the SENT specimens of THS steel.

Table 3
Fractures toughness of the HSLA steel in SENT specimens calculated through normalization technique (NT) and elastic unloading compliance method (UC) according to BS 8571:2014 ($J_{0.2}$), ASTM E1820-17a (J_{Ic}) and BS 7448-4:1997 ($J_{0.2BL}$) [kJ/m^2].

Specimen	BS 8571:2014		ASTM E1820-17a		BS 7448:1997	
	NT	UC	NT	UC	NT	UC
HSLA 01	283	298	669	697	460	494
HSLA 02	308	292	707	803	549	528
Mean	296 ± 18	295 ± 04	688 ± 27	750 ± 75	505 ± 63	511 ± 24

Table 4
Fractures toughness of the THS steel in SENT specimens calculated through normalization technique and elastic unloading compliance method according to BS 8571:2014 ($J_{0.2}$), ASTM E1820-17a (J_{Ic}) and BS 7448-4:1997 ($J_{0.2BL}$) [kJ/m^2].

Specimen	BS 8571:2014		ASTM E1820-17a		BS 7448:1997	
	NT	UC	NT	UC	NT	UC
THS 01	576	482	1326	1188	941	761
THS 02	524	505	1266	1238	824	800
THS 03	620	562	1306	1355	943	928
THS 04	603	492	1280	1354	914	817
THS 05	662	491	1393	1314	1026	878
Mean	597 ± 51	506 ± 32	1314 ± 50	1290 ± 74	930 ± 72	837 ± 66

compliance according to the three mentioned standards: BS 8571:2014, ASTM E1820–17a, and BS 7448-4:1997.

4. Discussion

4.1. Normalization method applied to SENT specimens

The applicability of normalization method in SENT geometry makes this methodology very attractive because of the lower sensitivity of elastic unloading compliance of SENT geometries compared to the SE(B) and C(T) ones, still lower for shallow cracks.

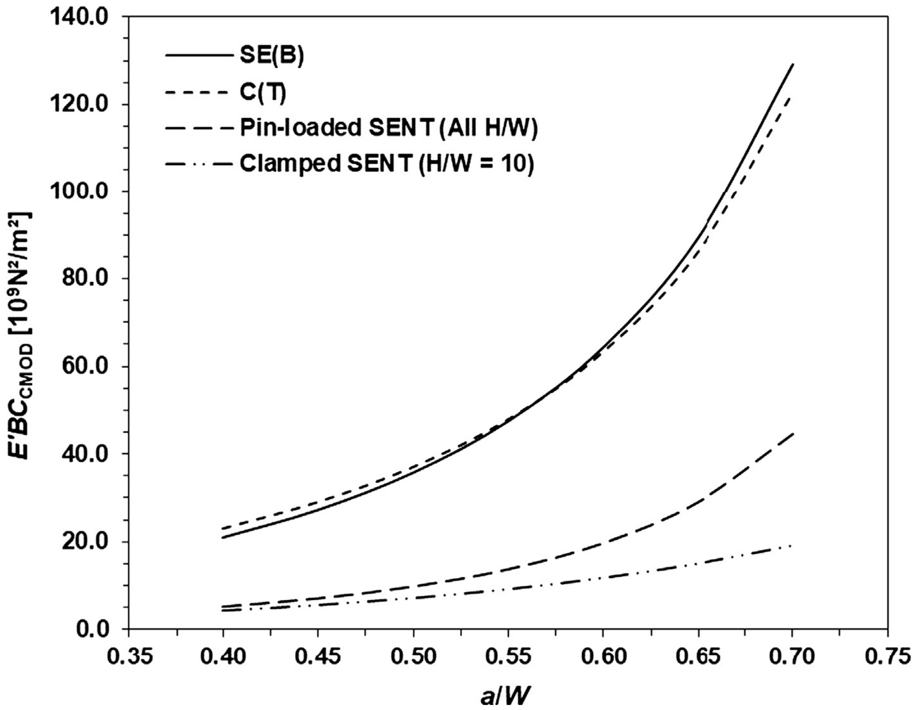

Fig. 13. a/W vs. $E'BC_{\text{CMOD}}$ for SE(B), C(T), pin-loaded SENT, and clamped SENT geometries.

This fact can be better observed in Fig. 13, which compares the solutions for a/W vs. $E'BC$ from CMOD for SE(B), C(T), pin-loaded SENT, and clamped SENT geometries.

Besides the mechanical properties, environment and temperature, the material response during fracture tests depends on the triaxiality level at the crack tip, which means that it is dependent on specimen geometry, crack size (a/W), loading mode, etc. Different configurations can lead to different crack tip constraint levels and plastic deformation zones/patterns [30]. High-constraint

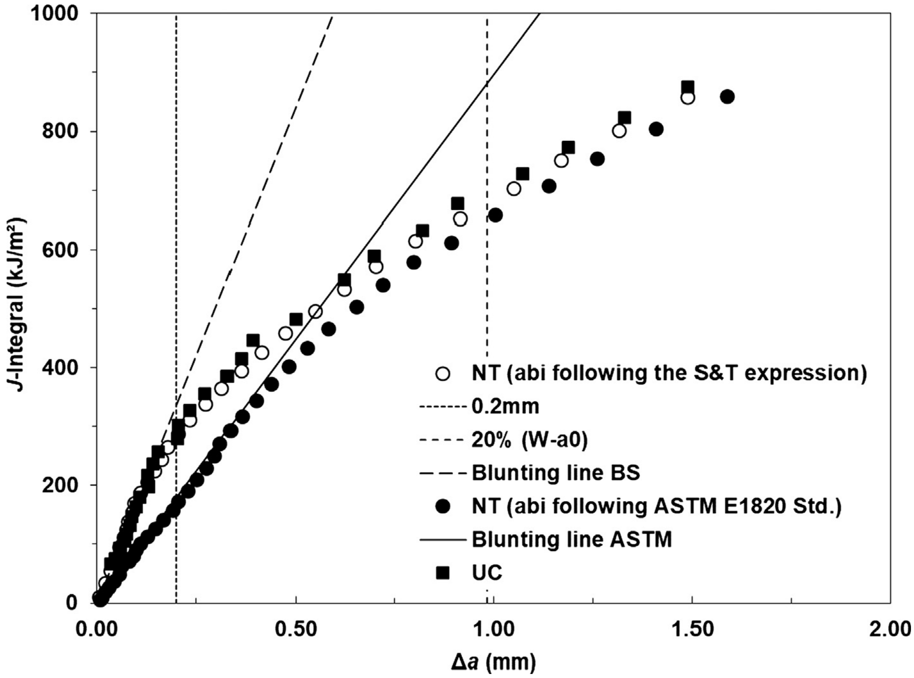

Fig. 14. J-R curves by normalization method calculated using m factor from Shen & Tyson, from ASTM E1820-17a standard, and by elastic compliance.

specimens, such as deeply cracked SE(B), C(T) and DC(T) specimens, limit plasticity to a region near the crack tip, at the remaining ligament. On the other hand, low-constraint specimens, as SENT and shallow cracked SE(B), are capable of deforming plastically more than high-constraint specimens and they do not restrict the plasticity to a limited region at the crack tip. When SENT specimens are loaded, they promote different plastic deformation patterns which include plastic deformation within and outside the remaining ligament. However, the use of CMOD allows us to accurately measure the displacement associated with the fracture process avoiding other plastic deformation contributions. Besides that, the η_{pl} factor that relates the plastic contribution of J-Integral to the work per

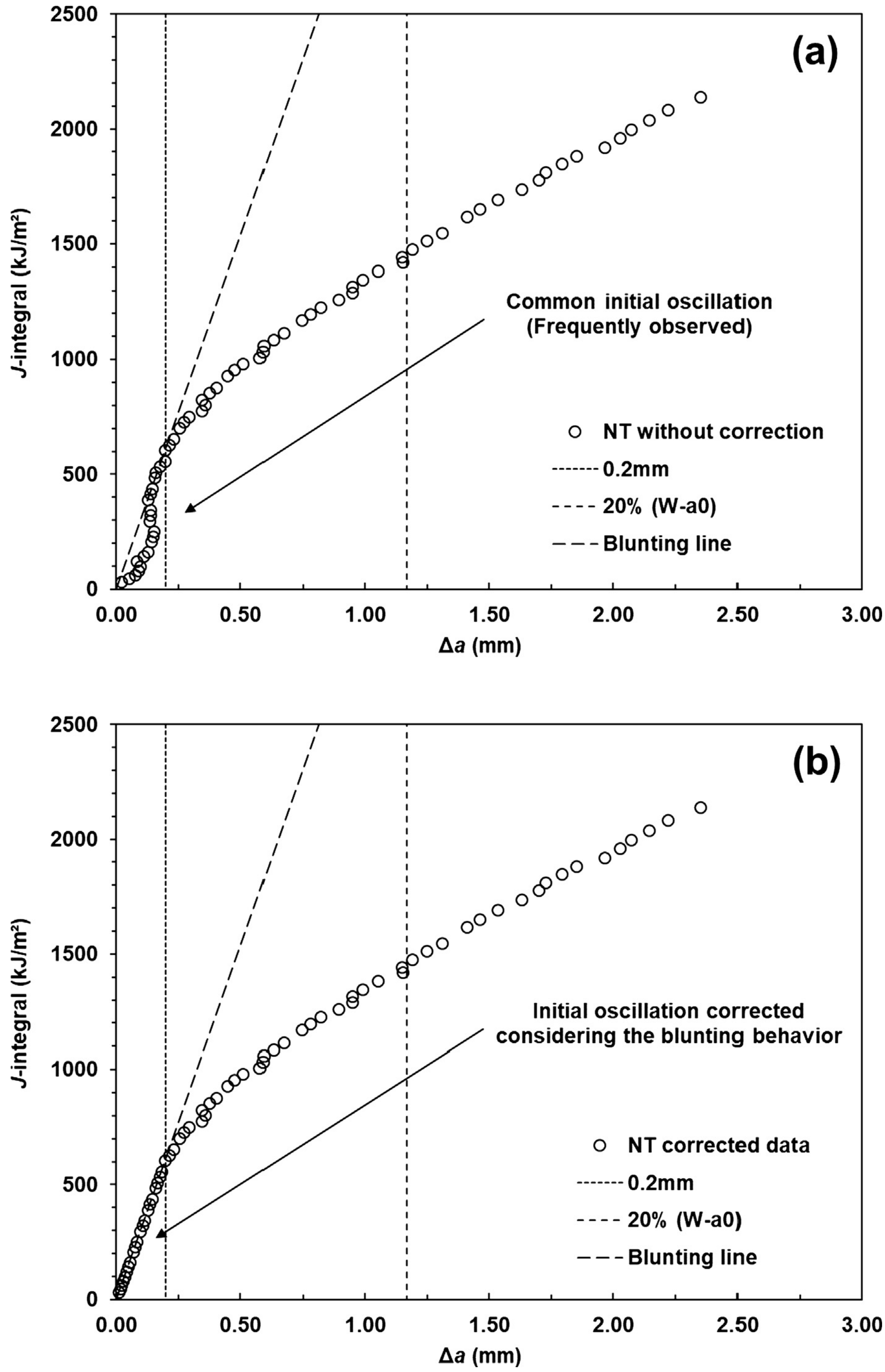

Fig. 15. Correction procedure for the initial oscillations in J-R curves measured through the normalization method. (a) Original J-R curve - common initial oscillations. (b) Corrected J-R curve.

unit uncracked ligament area must be derived from CMOD record as reported in some researches [30–32]. In this context, and as described earlier, the normalization method was applied based on P-CMOD records.

The crack length estimation procedure of the normalization method needs a blunting corrected crack size (a_{bi}). The concept of blunting line is not considered in the BS 8571:2014 standard and was introduced as [33]:

$$J = 2m\sigma_Y \Delta a, \quad (12)$$

where m is a constraint factor dependent on a/W, the stress state, and σ_{YS}/σ_{UTS} among others. For bending geometries, ASTM E1820-17a standard uses $m = 1$ in the blunting line slope and in the normalization method procedure [4], while BS 7448-4:1997 uses $m = 3.75/2$. It is important to note that there is no agreement in the literature about the value of m [33,34]. Instead, Shen & Tyson proposed the following equations to estimate the m value for clamped SENT geometries [35]:

$$m = A_1 \frac{a}{W} + A_2, \quad (13)$$

where

$$\begin{cases} A_1 = -0.1293 + 0.1152n - 0.00986n^2 + 0.000263n^3 \\ A_2 = 3.08670 - 0.2970n + 0.01940n^2 - 0.000427n^3 \end{cases}, \quad (14)$$

and n is the Ramberg-Osgood strain hardening exponent. In our case, Eq. (13) led to a blunting line slope that is very close to that used in BS 7448-4:1997 standard. Additionally, as can be seen in Fig. 14, the obtained normalization J-R curve (open circles) was very close to the unloading compliance one (dark squares). In opposition, the normalization J-R curve obtained by using ASTM E1820-17a blunting line ($m = 1$) (dark circles) did not match the unloading compliance well, as can also be seen in the same figure.

Another feature observed during the application of this technique is the initial oscillation of the J-R curve. Fig. 15a shows these oscillations for a SENT specimen of THS steel. These oscillations were observed in all J-R curves measured by the normalization method. They occur because of the crack length estimation through this methodology is very sensitive to the quality of the four parameters function (Eq. (6)), even more so for small amounts of plastic displacements [36]. A suggested procedure to correct this problem is to use the blunting line representing the crack tip blunting and shift all displaced $J - \Delta a$ data to this line. Fig. 15b presents the corrected J-R curve according to this procedure. All measured J-R curves presented in this investigation (Figs. 9–12) were corrected using this procedure. It is important to note that these oscillations occurred only in the initial part of the curves for small values of plastic displacement and out of the qualification region for the J-R curve determination (see Fig. 15a).

4.2. Crack extension

As can be seen in Figs. 7 and 8, the crack extension values obtained through normalization and elastic unloading compliance are in good agreement, falling close to the identity line. As can be seen in Table 2, unloading compliance underestimated final crack extension in some cases, but always within the limit imposed by ASTM E1820-17a and BSI 7448-4 standards [4,5].

4.3. Initiation fracture toughness

Normalization and unloading compliance methodologies led to similar initiation fracture toughness values. The maximum difference observed was approximately 20%. Tables 3 and 4 present these values. By comparing the crack initiation toughness mean values we can observe that the values obtained by the normalization method for the HSLA steel were in general smaller than values obtained by the elastic unloading compliance method. Besides, the opposite behavior was verified for the THS steel.

The experimental J-R curves obtained by both methodologies are in close agreement, as can be seen in Figs. 11 and 12. The crack propagation parameter $J_{1.0}$ presented similar values in all cases, as well as the corresponding slopes, ($dJ/da|_{1.0}$). This is another evidence that the normalization method using P-CMOD record for SENT specimens can be applied to measure J-R curves and to determine the initiation fracture toughness of the material.

Although only J-R curves were considered in this work, the proposed methodology with small modifications could be applied also to determination of CTOD-R curves, that are also considered in the BS 8571:2014 standard.

5. Concluding remarks

The normalization method proved to be a good alternative for J-R curve determination using SENT specimens with $0.4 < a_0/W < 0.55$ of two different structural steels. Crack length estimations and J-R curves by normalization and unloading compliance were in close agreement.

The following aspects need to be taken into account when the normalization method is applied to SENT specimens:

- The use of P-CMOD records allows us to accurately measure the displacement associated with the fracture process, avoiding other plastic deformation contributions;
- A blunting line slope based on the Shen & Tyson expression was introduced. This value was close to that given by BS 7448-4:1997.

Acknowledgments

To Egon R. Delgado Ramirez for the technical assistance. To CAPES for the M.Sc. scholarship of João T. O. de Menezes.

Appendix A. Supplementary material

Supplementary data associated with this article can be found, in the online version, at http://dx.doi.org/10.1016/j.engfracmech.2018.06.033.

References

[1] Hancock JW, Reuter WG, Parks DM. Constraint and toughness parameterized by T, constraint effects in fracture. ASTM STP 1171; 1993. p. 21–40.
[2] Joyce JA, Hackett EM, Roe C. Effect of crack depth and mode of loading on the J-R curve behavior of a high-strength steel, constraint effects in fracture. ASTM STP 1171; 1993. p. 239–63.
[3] Joyce JA, Link RE. Effects of constraint on upper shelf fracture toughness. Fracture mechanics. ASTM STP 1256 1995; 26: p. 142–77.
[4] ASTM E1820-17a. Standard test method for measurement of fracture toughness. ASTM International, West Conshohocken, PA; 2017, www.astm.org.
[5] BS 7448-4:1997. Fracture mechanics toughness tests - Part 4. Method for determination of fracture resistance curves and initiation values for stable crack extension in metallic materials. In: BSI Standards Publication; 2003.
[6] Nyhus B, Polanco ML, Orjasether O. SENT specimens an alternative to SENB specimens for fracture mechanics testing of pipelines. In: Proceedings of OMAE03, 22nd international conference on offshore mechanics and arctic engineering. Mexico; 2003. p. 259–66.
[7] Cravero S, Ruggieri C. Correlation of fracture behavior in high pressure pipelines with axial flaws using constraint designed test specimens - Part I: plane strain analyses. Eng Fract Mech 2005;72:1344–60.
[8] Cravero S, Bravo RE, Ernst HA. Constraint evaluation and effects on J-R resistance curves for pipes under combined load conditions. In: International society of offshore and polar engineers, 18th international offshore and polar engineering conference. Vancouver, Canada; 2008. p. 149–56.
[9] DNV Recommended Practice DNV-RP-F108. Fracture control for pipeline installation methods introducing cyclic plastic strain. Norway: Det Norske Veritas; 2006.
[10] Shen G, Gianetto JA, Tyson WR. Development of procedure for low constraint toughness testing using a single-specimen technique. MTL Report No.2008-18(TR).
[11] Shen G, Gianetto JA, Tyson WR. Measurement of J-R curves using single specimen technique on clamped SE(T) specimens. In: International society of offshore and polar engineers, 19th international offshore and polar engineering conference. Osaka, Japan; 2009. p. 92–99.
[12] Park D-Y, Tyson WR, Gravel J-P. Canmet SENT test method, updates and applications. Int J Press Vessels Pip 2017;156:8–16.
[13] BS 8571:2014. Method of test for determination of fracture toughness in metallic materials using single edge notched tension (SENT) specimens. In: BSI Standards Publication; 2014.
[14] Ernst HA, Paris PC, Rossow M, Hutchinson JW. Analysis of load-displacement relationships to determine J-R curve and tearing instability material properties, fracture mechanics. ASTM STP 677; 1979. p. 581–99.
[15] Herrera R, Landes JD. A direct J-R curve analysis of fracture toughness tests. J Test EvalJTEVA 1988;16:427–49.
[16] Paris PC, Ernst H, Turner CE. A J-integral approach to development of η-factors, fracture mechanics: Twelfth Conference, ASTM STP 700; 1980. p. 338–51.
[17] Joyce JA, Ernst H, Paris PC. Direct evaluation of J-resistance curves from load displacement records, fracture mechanics: twelfth conference, ASTM STP 700; 1980. p. 222–36.
[18] Ernst HA, Paris PC, Landes JD. Estimations on J-integral and tearing modulus T from a single specimen test record, fracture mechanics: thirteenth conference, ASTM STP 743; 1981. p. 476–502.
[19] Herrera R, Landes JD. Direct J-R curve analysis: a guide to the methodology, ASTM STP 1074; 1990. p. 24–43.
[20] Landes JD, Zhou Z, Lee K, Herrera R. Normalization method for developing J-R curves with the LMN function. J Test Evaluat, JTEVA 1991;19:305–11.
[21] Zhou Z, Lee K, Herrera R, Landes JD. Normalization: an experimental method for developing J-R curves, elastic-plastic fracture test methods: the user's experience (Second Volume). ASTM STP 1114 1991; 2: p. 42–56.
[22] Lee K, Landes JD. Developing J-R curves without displacement measurement using normalization. ASTM STP 1189; 1993. p. 133–67.
[23] Joyce JA. Analysis of a high rate round robin based on proposed annexes to ASTM E 1820. J Test Evaluat, JTEVA 2001;19:329–51.
[24] Zhu XK, Joyce JA. J-resistance curves testing of HY80 steel using SE(B) specimens and normalization method. Eng Fract Mech 2007;74:2263–81.
[25] Zhu XK, Lam PS, Chao YJ. Application of normalization method to fracture resistance testing for storage tank A285 carbon steel. Int J Press Vessels Pip 2009;86:669–76.
[26] Bergant MA, Yawny AA, Ipiña JEP. Experimental determination of J-resistance curves of nuclear steam generator tubes. Eng Fract Mech 2016;164:1–18.
[27] ASTM E8/E8M-15a. Standard test methods for tension testing of metallic materials. In: ASTM Book of Standards; 2016. p. 1–27.
[28] Cravero S, Ruggieri C. Estimation procedure of J-resistance curves for SE(T) fracture specimens using unloading compliance. Eng Fract Mech 2007;74:2735–57.
[29] BS 7448:1991. Fracture mechanics toughness tests. Method for determination of KIC, critical CTOD and critical J values of metallic materials. London: BSI British Standards Institution; 1999.
[30] Ruggieri C. Low constraint fracture toughness testing using SE(T) and SE(B) specimens. Int J Press Vessels Pip 2017;156:23–39.
[31] Kirk MT, Dodds RH. J and CTOD estimation equations for shallow cracks in single edge notch bend specimens. J Test Eval 1993;21:228–38.
[32] Zhou DW. Measurement of J-R curves for low-constraint specimens. Eng Fract Mech 2011;78:605–22.
[33] Landes JD. The blunting line in elastic-plastic fracture. Fatigue Fract Eng Mater Struct 1995;18:1289–97.
[34] ISO 12135. Metallic materials – unified method of test for the determination of quasistatic fracture toughness. International Standards Organization; 2016.
[35] Shen G, Tyson WR. Evaluation of CTOD from J-integral for SE(T) specimens. In: Pipelines international, 5th pipeline technology conference and exhibition. Ostend, Belgium; 2009.
[36] Scibetta M, Lucon E, Schuurmans J, van Walle E. Numerical simulations to support the normalization data reduction technique. Eng Fract Mech 2006;73:524–34.